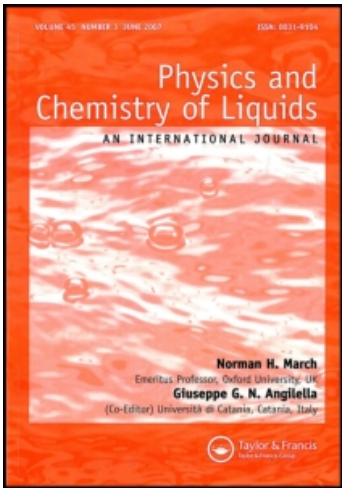

Physics and Chemistry of Liquids
Publication details, including instructions for authors and subscription information:
http://www.informaworld.com/smpp/title~content=t713646857

Simplified RPA Bhatia—Young Calculations of the Phase Diagram for a Model Binary Mixture. I. Equal Size Molecules

S. M. Osman[ab]; M. Silbert[cd]
[a] International Centre for Theoretical Physics, Trieste, Italy [b] Department of Physics, Faculty of Science, Ain Shams University, Cairo, Egypt [c] Departamento de Fisica Teórica, Facultad de Ciencias, Universidad de Valladolid, Valladolid, Spain [d] School of Physics, University of East Anglia, Norwich, UK

To cite this Article Osman, S. M. and Silbert, M.(1991) 'Simplified RPA Bhatia—Young Calculations of the Phase Diagram for a Model Binary Mixture. I. Equal Size Molecules', Physics and Chemistry of Liquids, 23: 4, 239 — 250
To link to this Article: DOI: 10.1080/00319109108027260
URL: http://dx.doi.org/10.1080/00319109108027260

Phys. Chem. Liq., 1991, Vol. 23, pp. 239–250
Reprints available directly from the publisher
Photocopying permitted by license only

SIMPLIFIED RPA BHATIA–YOUNG CALCULATIONS OF THE PHASE DIAGRAM FOR A MODEL BINARY MIXTURE. I. EQUAL SIZE MOLECULES

S. M. OSMAN[1]

International Centre for Theoretical Physics, Trieste, Italy.

and

M. SILBERT[2]

Departamento de Fisica Teórica, Facultad de Ciencias, Universidad de Valladolid, E-47011 Valladolid, Spain.

(Received 10 August 1990)

We present the results of calculations of the phase diagram for a model binary mixture of equal size hard-core molecules interacting via square-well potentials, but assuming that the system does not satisfy Berthelot rule. In particular, we analyse the effects that the parameter which measures departures from this rule has on the phase diagram of the system. The calculations are based on the Bhatia–Young model for the bulk properties of liquid mixtures.

KEY WORDS: Mixtures, random phase approximation.

1 INTRODUCTION

We have recently presented the results of calculations of the density profiles and surface tension for a particular phase diagram of a model binary mixture[1]. There we made reference to the rich variety of phase diagrams which may be obtained by the appropriate choice of the parameters of the potentials. In this work we present a subset of them, namely those which are obtained by assuming: a) the sizes of the molecules in both components are the same; and b) two particular choices for the parameters of the potentials.

In our calculations we have used the simplified RPA Bhatia–Young model[2] which proposes a simple expression for the free energy of mixing of a binary fluid—from which we obtain expressions for the other thermodynamic properties of interest—using hard spheres as a reference system and a tail interaction between the components. The advantages of this approach lie in the simplicity of the expressions obtained for the properties of interest and that, at this level of description, the details of the potential are not important; only the parameters of the potentials are. Thus any set of potentials described by the same set of parameters will predict, within this

[1] Permanent address: Department of Physics, Faculty of Science, Ain Shams University, Cairo, Egypt.
[2] On Study Leave from the School of Physics, University of East Anglia, Norwich NR4 7TJ, UK.

formalism, the same results. Nonetheless we visualize the attractive potentials by means of square well tails which, for the choice made for our calculations, read

$$v_{ij}(r) = \begin{cases} 0 & r < \sigma \\ -\varepsilon[(1-\alpha)\delta_{ij} + \alpha] & \alpha < r < \lambda\sigma \\ 0 & r > \lambda\sigma \end{cases} \tag{1.1}$$

where δ_{ij} denotes the Kronecker delta.

In Eq. (1.1) we have assumed $\sigma_{11} = \sigma_{22} = \sigma_{12} \equiv 1/2(\sigma_{11} + \sigma_{22}) = \sigma$. Also α denotes departures from Berthelot rule, i.e. the non-additivity of the potential tails; $\varepsilon_{11} = \varepsilon_{22} = \varepsilon$; $\varepsilon_{12} = \alpha\varepsilon$. Actually this is the same potential used by Ichimura and Ueda[3] in their calculations of the phase diagram and chemical potential surfaces using the Leonard–Barker–Henderson[4,5] thermodynamic perturbation theory.

For the potential given by Eq. (1.1) values of $\alpha > 1$ lead to compound forming tendencies, whereas $\alpha < 1$ produces tendencies to phase separation in the binary mixture. We shall examine the behaviour of the latter case for two values of α.

The layout of the paper is as follows. In Section 2 we sketch the formalism used in this work. The results for the concentration fluctuations, phase diagram and chemical potential surfaces are presented in Section 3; finally in Section 4, we discuss briefly our results

2 METHOD

Within the RPA Bhatia–Young model, the Helmholtz free energy per atom, f, is given by

$$f = f_{\mathrm{HS}} + \tfrac{1}{2}\tilde{v}_{ij}(0) \tag{2.1}$$

where f_{HS} denotes the free energy per atom of the hard spheres reference system. In the calculations reported below we use the results for f_{HS} obtained from the compressibility route in the Percus–Yevick approximation[6]. $\tilde{v}_T(0)$ is the long wavelength limit of the Fourier transform (FT) of the potential tail,

$$\tilde{v}_T(0) = \tfrac{1}{2}\rho \sum_{i,j} x_i x_j \tilde{v}_{ij}(0) \tag{2.2}$$

where ρ is the number density, x_i the concentration of component i, such that $x_1 + x_2 = 1$, and

$$\tilde{v}_{ij}(0) = \int dr\, v_{ij}(r)$$

is the FT of $v_{ij}(r)$ in the limit $k = 0$.

For the potentials given by Eq. (1.1)

$$\beta\tilde{v}_T(0) = \frac{K}{T}\eta\{x^2 + (1-x)^2 + 2\alpha x(1-x)\} \tag{2.3}$$

In Eq. (2.3) $x \equiv x_1$; $\eta = (1/6)\pi\rho\sigma^3$ denotes the packing fraction of atoms with diameters α; $\beta \equiv (k_B T)^{-1}$ where k_B is the Boltzmann constant and T the temperature; and

$$K = -\frac{4\varepsilon(\lambda^3 - 1)}{k_B}$$

Other thermodynamic properties of interest follow from f. Thus the pressure is given as

$$P = P_{\mathrm{HS}} + \tfrac{1}{2}\rho\tilde{v}_T(0) \tag{2.4}$$

The Gibbs free energy per atom, g, reads

$$g = g_{\mathrm{HS}} + \tilde{v}_T(0) \tag{2.5}$$

from which we obtain the chemical potentials

$$\mu_1 = g + (1 - x)\left(\frac{\partial g}{\partial x}\right)_{T,P}; \qquad \mu_2 = g - x\left(\frac{\partial g}{\partial x}\right)_{T,P} \tag{2.6}$$

Finally, another property we shall examine is the long wavelength limit of the Bhatia–Thornton concentration–concentration partial structure factor[7]

$$S_{cc}(0) = \left(\beta \frac{\partial^2 g}{\partial^2 x}\right)^{-1}_{T,P} \tag{2.7}$$

which, from Eq. (2.5), may be written as

$$S_{cc}^{-1}(0) = S_{cc}^{\mathrm{HS}-1}(0) + S_{cc}^{T-1}(0) \tag{2.8}$$

We note that, within this approach, Eqs. (2.1), (2.4), (2.6) and (2.7) may be written in close analytic form.

The determination of the phase diagram for the binary mixture requires, at each temperature, the solution of the following three coupled equations

$$\begin{aligned} P^{\mathrm{I}}(\rho, x, T) &= P^{\mathrm{II}}(\rho, x, T) \\ \mu_1^{\mathrm{I}}(\rho, x, T) &= \mu_1^{\mathrm{II}}(\rho, x, T) \\ \mu_2^{\mathrm{I}}(\rho, x, T) &= \mu_2^{\mathrm{II}}(\rho, x, T) \end{aligned} \tag{2.9}$$

where I and II specify each of the coexisting phases.

3 RESULTS

The results reported below are given in reduced units in terms of the potentials parameters σ and ε. Thus $\rho^* = \rho\sigma^3$; $T^* = k_B T/\varepsilon$; $\mu^* = \mu/\varepsilon$; and $P^* = P\alpha^3/\varepsilon$ denote the reduced density, temperature, chemical potential and pressure, respectively. In all our calculations we have used $\lambda = 1.5$.

3.1 *Concentration–concentration fluctuations*

In Figure 1 we present the results for $T^* = 0.8$ and two values of α: (a) 0.6 and (b) 0.8, for several values of the pressure P^*. We show, in Figure 1(b), how increasing pressures inhibit concentration fluctuations. At $P^* \geq 0.12$, $S_{cc}(0)$ takes on values below its ideal behaviour, $x(1-x)$; namely preferred homocoordination is forced upon the mixture. At lower pressures, for values of $P^* \leq 0.06$ the system exhibits a miscibility gap over a wide range of concentrations. The change of the non-additivity parameter α from 0.8 to 0.6 results in phase separation already taking place at the much higher pressure of $P^* = 0.20$, as shown in Figure 1(a).

3.2 *Phase diagram*

We have solved Eq. (2.9) for the same values of T^* and α as in Section 3.1 for different values of P^*. For each T^* and P^* the equation of state determines the isothermal-isobaric relation, of which a typical example is shown in Figure 2. Below a critical line all isobars have three branches showing three distinct regions for the gas, liquid and unstable regions. The curve with the broken line shows the liquid–gas coexistence curve. Below this curve the dotted lines separate the gas, liquid and unstable regions. In Figure 2(a) the circles show a liquid–liquid coexistence region at this particular temperature; this region is no longer present when the non-additivity parameter is increased to 0.8.

In Figure 3 we present the results for the chemical potentials as a function of concentration. Because of the choice of equal size diameters, there is a symmetry of results with respect to equimolar composition, and we therefore present our results in the composition range $0 \leq x \leq 0.5$. The behaviour of the $\mu - x$ phase diagram may be classified into four types: a) In Figure 3(a) we find liquid–gas coexistence. Here μ_1 and μ_2 show three branches—G, M, and L—which denote the gas, unstable and liquid phases respectively; b) critical behaviour (positive azeotropy) around $x = 0.5$ as shown in Figure 3(b). The branch M disappears and the G and L branches joint smoothly at the critical point C; c) in Figure 3(c) μ_1 and μ_2 intersect at points L_1 and L_2 showing liquid–liquid coexistence as well as a van der Waals loop for the liquid–gas coexistence; and d) liquid–liquid coexistence at L_1 and L_2, as well as critical behaviour for the liquid–gas coexistence curve at point C, as shown in Figure 3(d).

In Figures 4 and 5 we present the results for the $P^* - x$ phase diagram for $\alpha = 0.6$ and 0.8, covering a wide range of temperatures. First, we discuss the case $\alpha = 0.8$. For $T^* \leq 0.62$ we find liquid–liquid immiscibility at high pressures, whereas the liquid–gas coexistence (which is difficult to identify) shows up at lower pressures, as shown in Figure 4(a). As the temperature is increased, the liquid–gas coexistence shows positive azeotropy[8] at P^*_{xz} and $x = 0.5$, as shown in Figures 4(b)–(g). For $T^* > 0.8$ the liquid–gas coexistence curve shows two critical points at pressure P^*_c, as seen in Figures 4(h)–(j). This is also the case for $\alpha = 0.6$, as shown in Figures 5(h)–(j). Liquid–liquid coexistence only appears for the lower value of the non-additivity parameter, $\alpha = 0.6$. Actually, in Figure 5(a) we find liquid–liquid immiscibility at high pressures, while liquid–liquid coexistence starts building up at lower

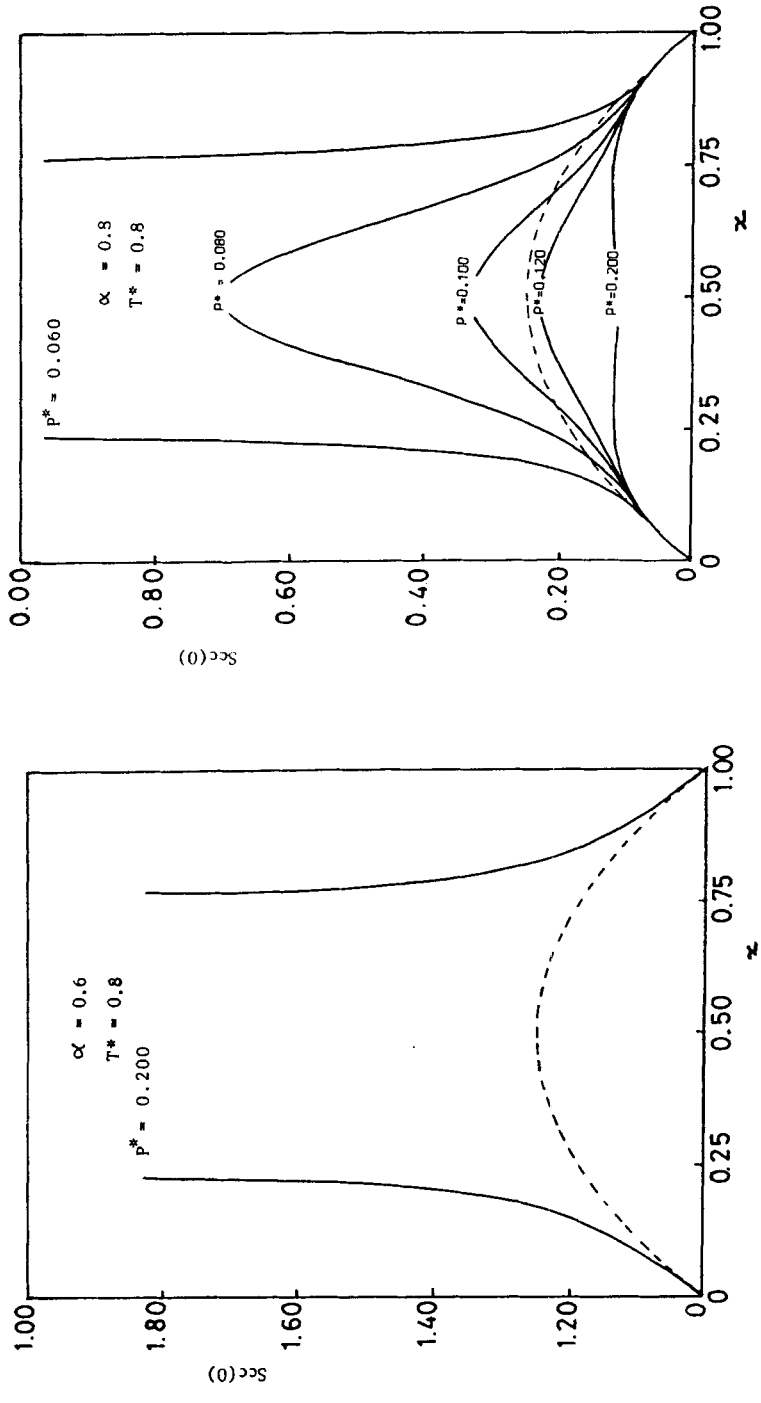

Figure 1 The long wavelength limit of the concentration–concentration partial structure factor $S_{cc}(0)$ as a function of concentration at $T^* = 0.8$ and different pressures. The dotted line denotes the ideal mixture result $S_{cc}(0) = x(1-x)$; (a) $\alpha = 0.6$; (b) $\alpha = 0.8$.

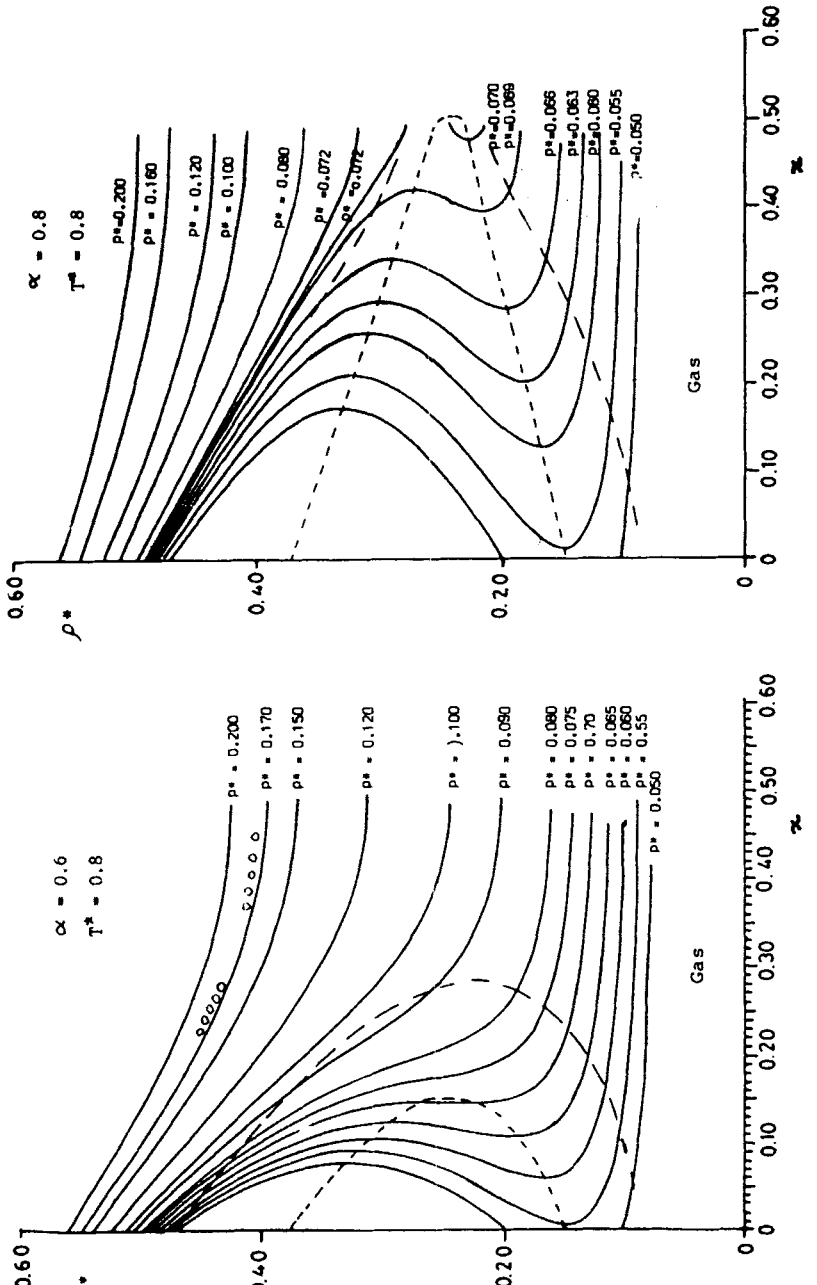

Figure 2 Isothermal-isobaric $\rho^* - x$ phase diagram at $T^* = 0.8$ and different pressures, as shown by the solid lines; the dotted line marks the boundary between the gas, liquid and unstable phases; the broken lines indicate the gas–liquid coexistence curve; the circles show the liquid–liquid coexistence region: (a) $\alpha = 0.6$; (b) $\alpha = 0.8$.

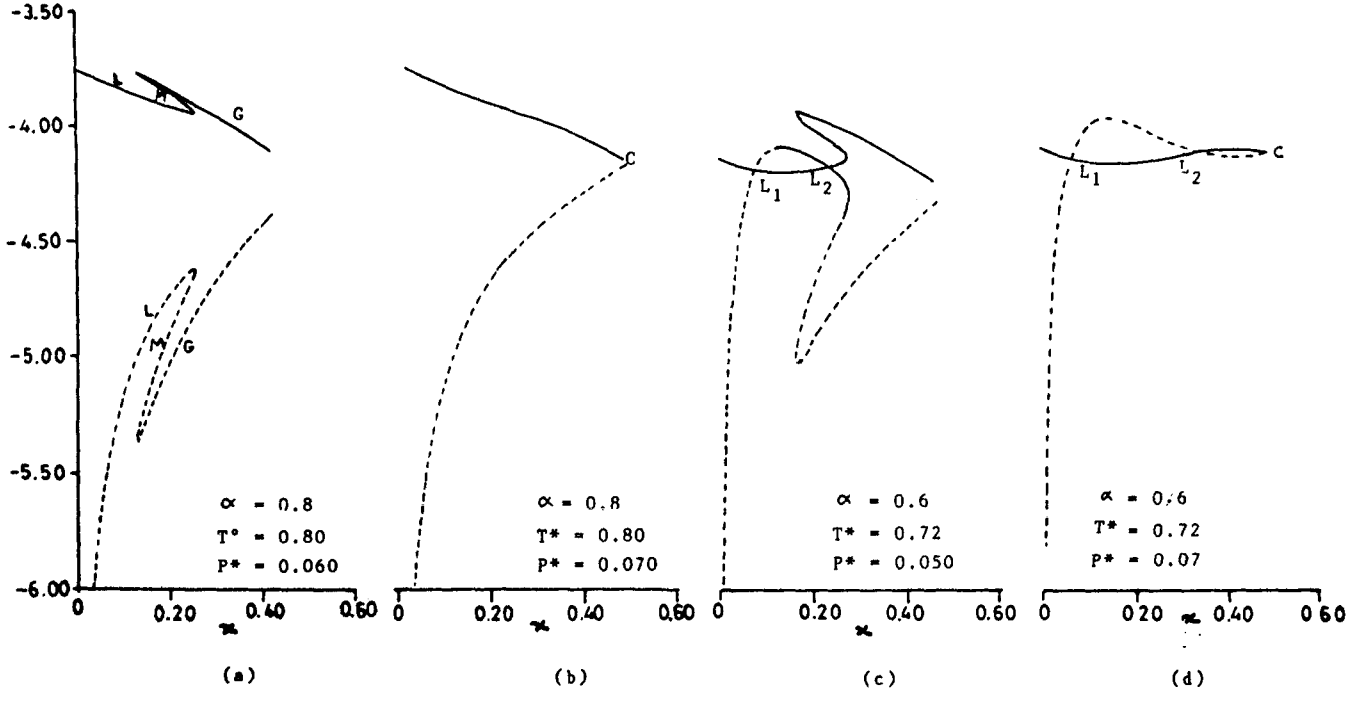

Figure 3 Chemical potentials for each component as a function of concentration. μ_1^*, dotted lines; μ_2^*, solid lines: (a) gas–liquid coexistence at $T^* = 0.8$, $P^* = 0.06$ and $\alpha = 0.8$; (b) critical point C at the end of the liquid–gas coexistence, at $T^* = 0.8$, $P^* = 0.06$ and $\alpha = 0.8$; (c) liquid–liquid coexistence at L_1 and L_2, as well as gas–liquid coexistence, at $T^* = 0.72$, $P^* = 0.05$ and $\alpha = 0.6$; (d) liquid–liquid coexistence at L_1 and L_2, and critical behaviour C at the end of the liquid–gas coexistence, at $T^* = 0.72$, $P^* = 0.07$ and $\alpha = 0.6$.

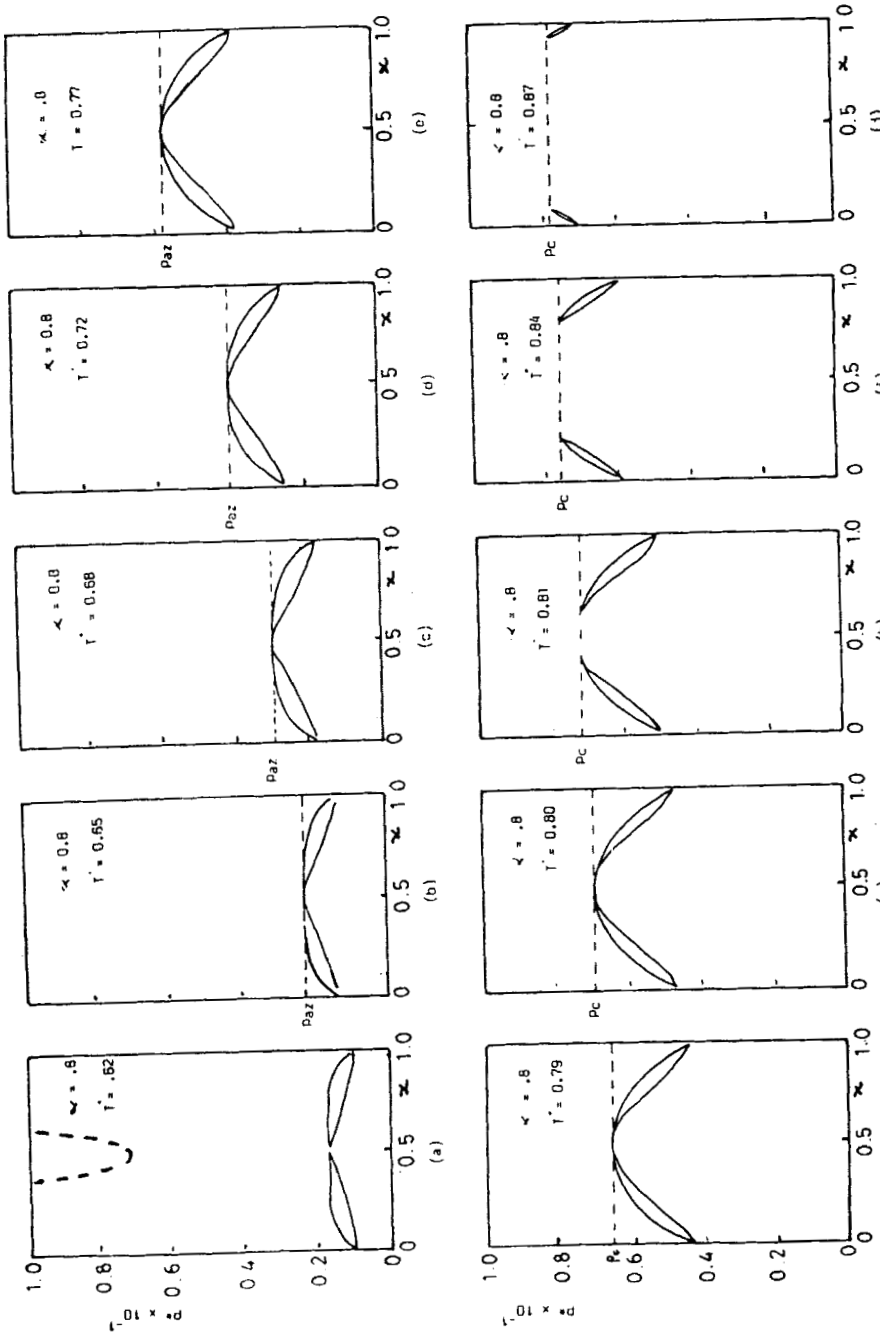

Figure 4 $P^* - x$ phase diagram for $\alpha = 0.8$ at ten different temperatures. Solid lines denote gas–liquid coexistence; broken lines denote liquid–liquid immiscibility.

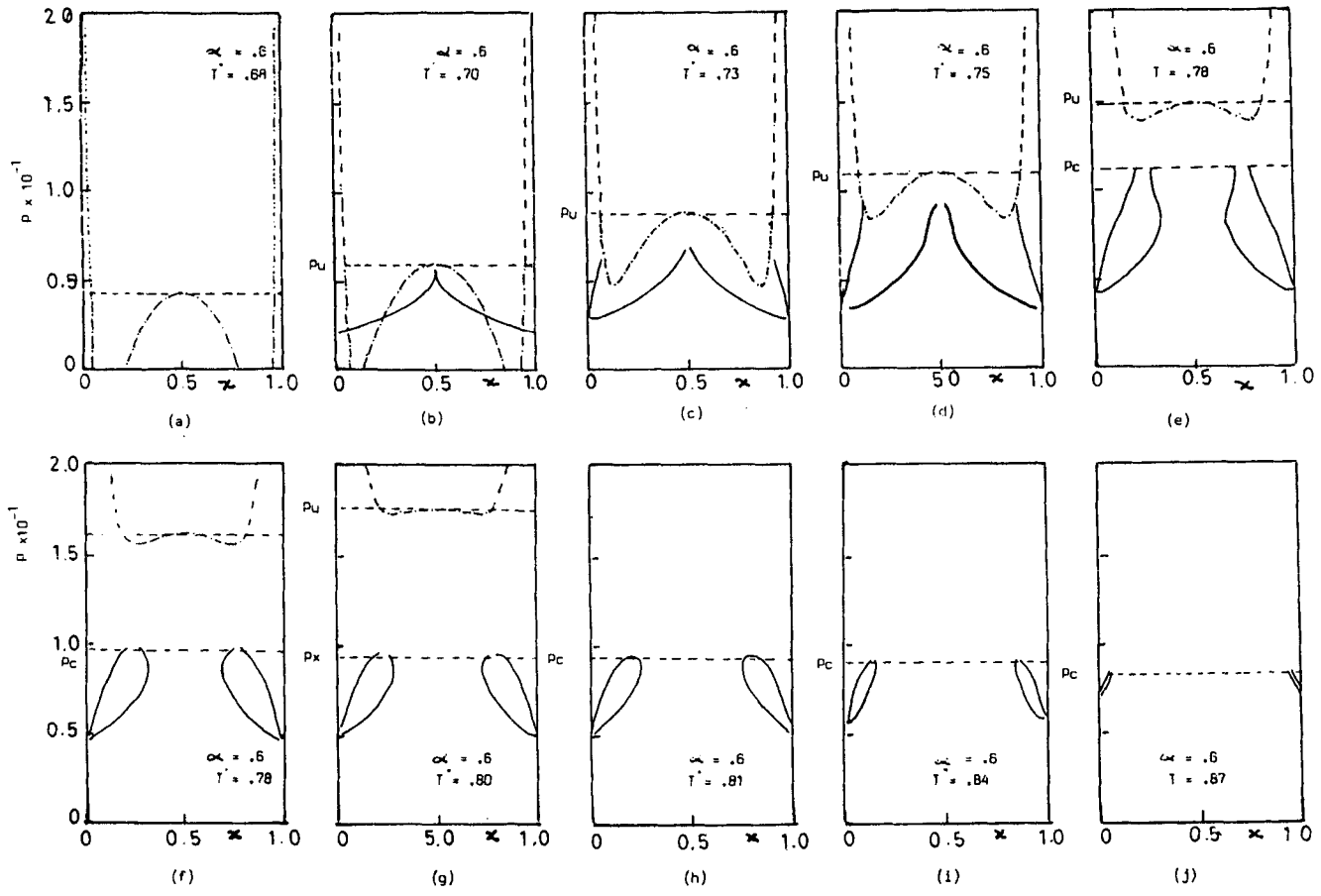

Figure 5 $P^* - x$ phase diagram for $\alpha = 0.6$ at ten different temperatures. Solid lines denote gas–liquid coexistence; dashed-dotted lines denote liquid–liquid coexistence; broken lines denote liquid–liquid immiscibility.

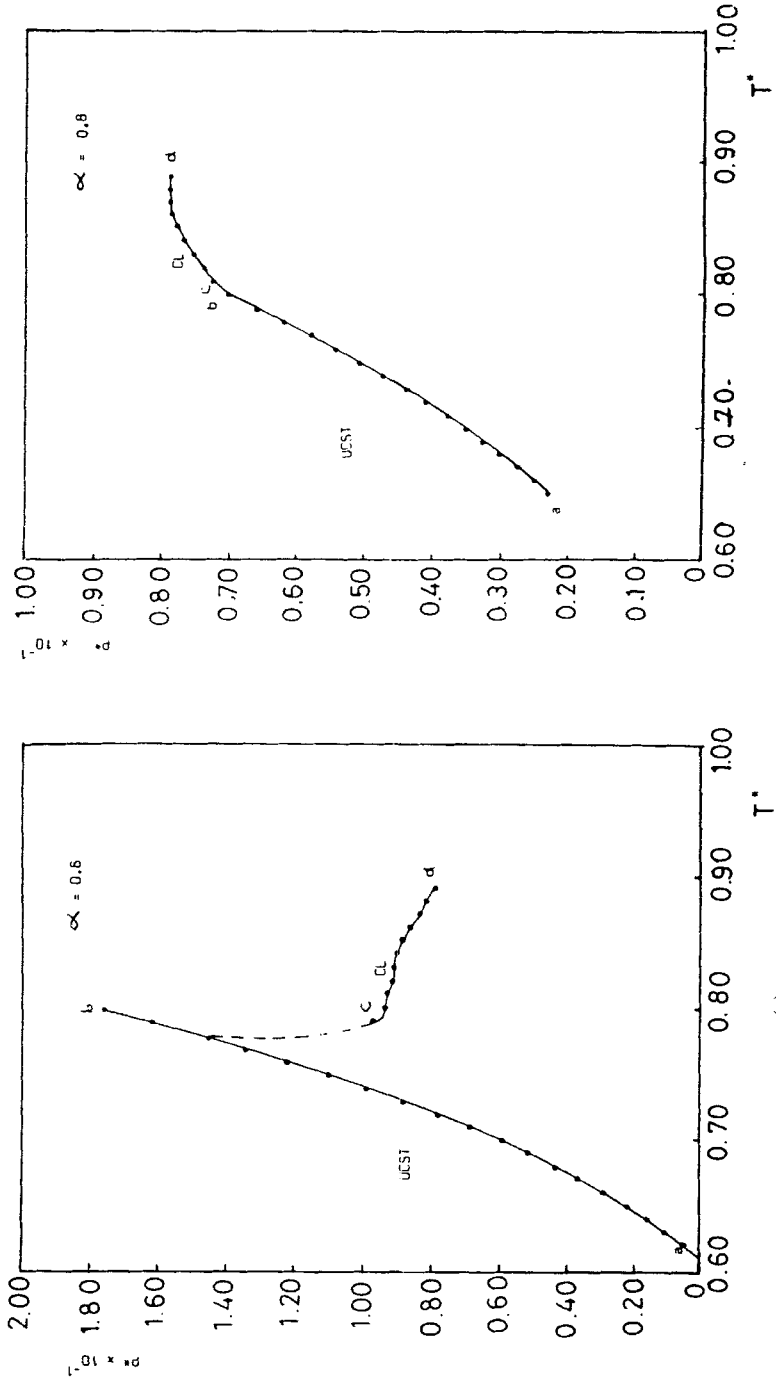

Figure 6 $P^* - T^*$ phase diagram. Section a–b shows the critical line of liquid–liquid equilibria (UCST); section c–d shows the critical line of gas–liquid coexistence (CL); the broken lines denote the values of CL extrapolated from the calculated results: (a) $\alpha = 0.6$; (b) $\alpha = 0.8$.

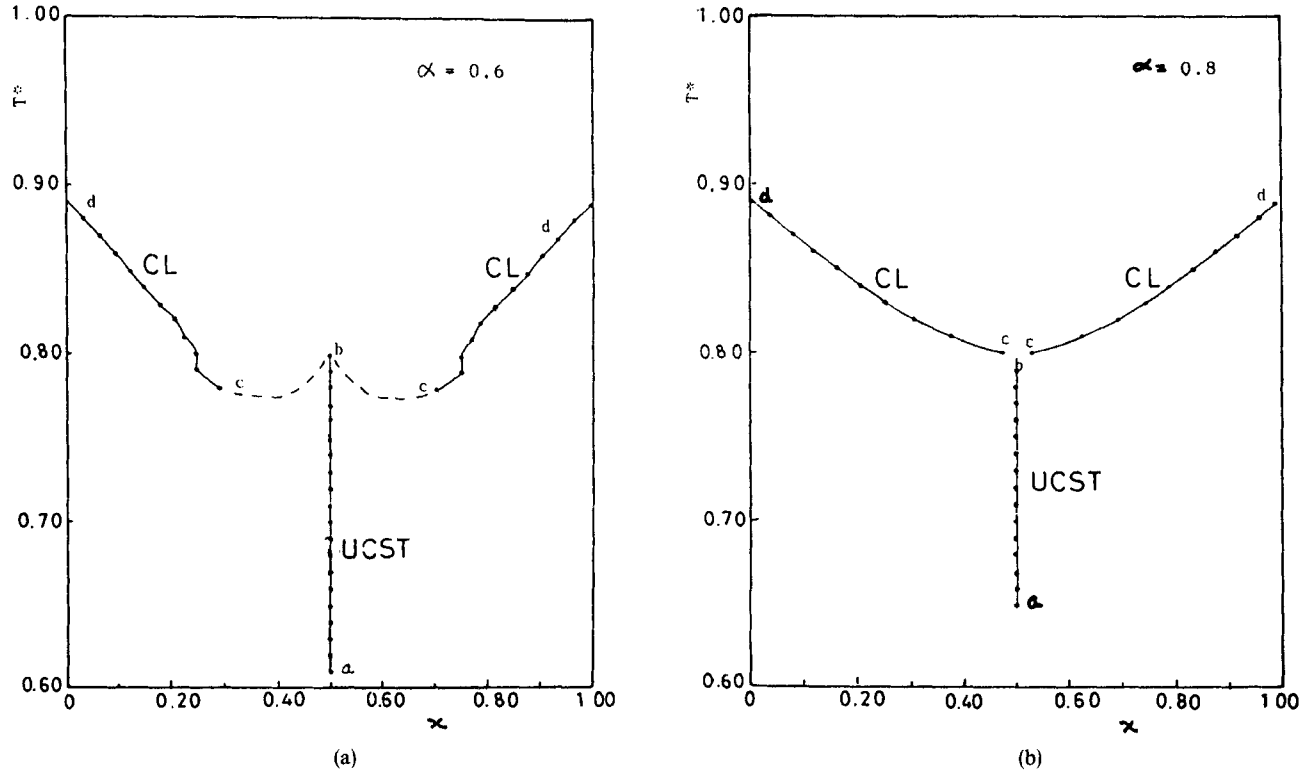

Figure 7 $T^* - x$ phase diagram. Section a–b shows the critical line of liquid–liquid equilibria (UCST); sections c–d show the critical line of gas–liquid coexistence (CL); the broken lines denote the values of CL extrapolated from the calculated results: (a) $\alpha = 0.6$; (b) $\alpha = 0.8$.

pressures. As the temperature is increased, the regions of liquid–liquid coexistence and liquid–gas coexistence overlap, as seen in Figure 5(b)–(d). At the same time liquid–liquid coexistence is pushed towards higher pressures until it disappears altogether, as shown in Figures 5(e)–(g).

The critical lines in the $P^* - T^*$ and $T^* - x$ planes are presented in Figures 6 and 7. For the case $\alpha = 0.8$ the liquid–gas critical line (CL) joins up the two critical points, and the azeotropic critical line (UCST) follows. The minimum temperature on the critical line is taken to be $T^* = 0.8$, and the maximum concentration is $x \cong 0.485$. In the temperature range $0.75 \leq T^* \leq 0.8$, for the case $\alpha = 0.6$, our model fails to detect the liquid–gas critical points within reasonable accuracy.

4 DISCUSSION

The results presented in the preceding section exhibit the rich variety of phase behaviour expected in binary mixtures, subject to the constraints of equal size diameters and values of the non-additivity parameters restricted to $0 < \alpha < 1$[9].

Our results are in very good qualitative agreement with those obtained by Ichimaru and Ueda[3], in those cases when they are comparable. This agreement gives us confidence in our approach, and suggests that it could be used to evaluate the bulk and surface properties of actual binary mixtures by a suitable parametrisation of the potential parameters—as we did for the one component case[10]—and using different size diameters. Work along these lines is in progress.

Acknowledgements

We are grateful to W. H. Young for his interest in this work. One of us (SMO) thanks the University of East Anglia for hospitality during a research visit when most of this work was carried out, and the ICTP at Trieste for his appointment as an Associate Member (1989–1995) where this work was completed. The other (MS) gratefully acknowledges the DGICYT of Spain for the provision of a Visiting Fellowship during which this work was written up.

References

1. S. M. Osman and M. Silbert, *J. Non-Cryst. Solids*, **117/118**, 646 (1990).
2. A. B. Bhatia and W. H. Young, *Phys. Chem. Liq.*, **14**, 47 (1984).
3. T. Ichimura and A. Ueda, *Mol. Phys.*, **42**, 733 (1981); *J. Chem. Phys.*, **74**, 3566 (1981).
4. P. J. Leonard, D. Henderson and J. A. Barker, *Trans. Faraday Soc.*, **66**, 2439 (1970); *Mol. Phys.*, **21**, 107 (1971).
5. B. A. Pailthorpe and D. A. McQuarrie, *Mol. Phys.*, **29**, 1333 (1975).
6. J. L. Lebowitz and J. S. Rowlinson, *J. Chem. Phys.*, **41**, 133 (1975).
7. L. J. Gallego, J. A. Somoza and M. Silbert, *Z. Naturforsch.*, **44a**, 793 (1989).
8. J. L. Rowlinson, *Liquids and Liquid Mixtures*, 2nd ed., (Butterworths: London, 1971).
9. R. L. Scott and P. H. van Konynenburg, *Discuss. Faraday Soc.*, **49**, 87 (1970).
10. S. M. Osman and M. Silbert, *Phys. Chem. Liq.*, **17**, 257 (1988).